Chapter 2
Natural Convective Heat Transfer from Short Cylindrical Cylinders Having Exposed Upper Surfaces and Mounted on Flat Adiabatic Bases

Keywords Natural convection · Cylinders · Cylindrical · Short · Numerical · Experimental · Inclined · Correlation equation · Isothermal

2.1 Introduction

Numerical and experimental results for natural convective heat transfer from short circular cylinders having an exposed upper surface will be considered in this chapter, this situation having been introduced in Chap. 1. The cylinders considered in all cases are mounted on a flat adiabatic base. Results for a vertical cylinder will first be considered and attention will then be turned to the case where the cylinder in set at an angle to the vertical. Attention in this chapter will be restricted to isothermal cylinders. Most of the results discussed in this chapter were obtained numerically but a limited number of experimental results will also be considered. In the last section of this chapter, the effect of having a flat adiabatic section mounted above the cylinder will be considered. Because the same basic geometry is considered in all sections of the chapter and because the same basic numerical and experimental methods were used in obtaining all of the results that are discussed in this chapter there is some overlap between the material in the various chapter sections.

The results presented in this chapter are mainly based on those given by Oosthuizen (2007), Scott and Oosthuizen (2000), Kalendar and Oosthuizen (2009), Kalendar et al. (2011), and Oosthuizen and Paul (2008).

2.2 Vertical Isothermal Cylinder

A numerical study of natural convective heat transfer from a vertical isothermal circular cylinder which has an exposed horizontal top surface will be discussed in this section (Oosthuizen 2007). In the considered situation, the exposed horizontal upper surface is maintained at the same temperature as the vertical cylindrical side wall of the cylinder. The cylinder is mounted on a flat horizontal adiabatic base

Fig. 2.1 Flow situation considered (Oosthuizen 2007, ASME Paper IMECE2007-42711. By permission)
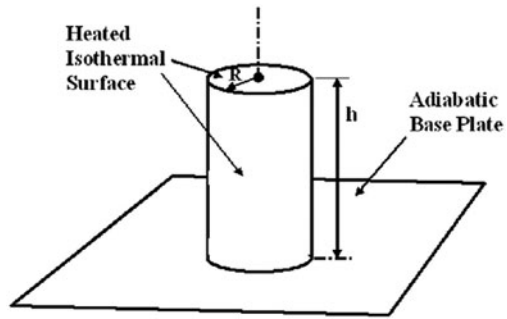

Fig. 2.2 Coordinate system used and definition of side and top surfaces (Oosthuizen 2007, ASME Paper IMECE2007-42711. By permission)
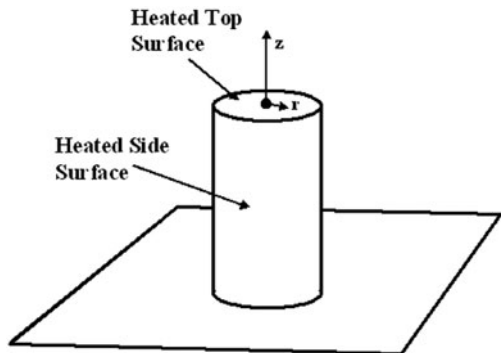

plate. Therefore, the flow situation considered is as shown in Fig. 2.1. Attention in this section is limited to the case where the cylinder points vertically upward. A comparison of the numerical results with some limited experimental results will also be discussed.

Under some circumstances, the heat transfer rate from the exposed horizontal upper surface of the cylinder can be neglected compared to that from the curved vertical side surface of the cylinder and in some circumstances the heat transfer rate from the curved surface can be adequately predicted using vertical flat plate equations, i.e., by ignoring curvature effects. The conditions under which these assumptions can be made will be considered here.

2.2.1   Solution Procedure

The flow has been assumed to be axisymmetric about the vertical cylinder axis and to be steady and laminar. It has also been assumed that the fluid properties are constant except for the density change with temperature which gives rise to the buoyancy forces, this being treated by using the Boussinesq approach. The coordinate system used in the analysis is shown in Fig. 2.2. As will be seen from this figure, the z-coordinate is measured vertically upward in the axial direction and the r-coordinate is measured in the radial direction.

Fig. 2.3 Solution Domain ABCDEFA (Oosthuizen 2007, ASME Paper IMECE2007-42711. By permission)
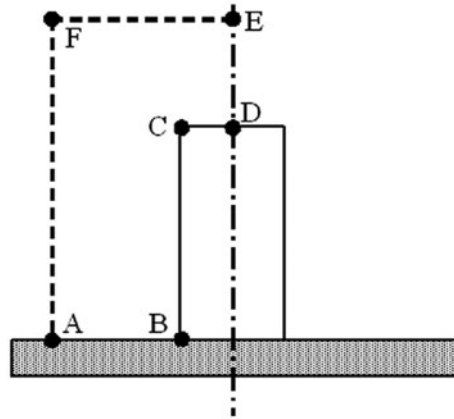
Because the flow has been assumed to be axisymmetric about the vertical center-line of the cylinder, the flow is two-dimensional and the domain used in obtaining the solution is as shown in Fig. 2.3.

Considering the surfaces shown in Fig. 2.3, since flow symmetry is being assumed, the assumed boundary conditions on the solution are:

$$\text{BCD:} \, u_z = 0, u_r = 0, T = T_W$$

$$\text{DE:} \, u_r = 0, \frac{\partial u_z}{\partial r} = 0, \frac{\partial T}{\partial r} = 0 \tag{2.1}$$

$$\text{AFE:} \, T = T_F, p = p_F$$

$$\text{AB:} \, u_z = 0, u_r = 0, \frac{\partial T}{\partial z} = 0$$

The governing equations subject to these boundary conditions were numerically solved using a commercial finite-element CFD solver. Once the solution was obtained the surface heat transfer rate was determined from the calculated temperature distribution. The heat transfer rate has been expressed in terms of a mean Nusselt number based on the height of the cylinder, h, and the overall temperature difference $(T_w - T_F)$, i.e., defined by:

$$Nu_{mc} = \frac{q'_{mc} h}{k(T_w - T_F)}, \tag{2.2}$$

where q'_{mc} is the mean heat transfer rate per unit area from the entire surface of the cylinder. Mean Nusselt numbers for the vertical cylindrical side surface of the cylinder and for the horizontal top surface of the cylinder have also been used, these being defined as follows:

$$Nu_{ms} = \frac{q'_{ms} h}{k(T_w - T_F)} \tag{2.3}$$

and

$$Nu_{mt} = \frac{q'_{mt}\, h}{k(T_w - T_F)},$$ (2.4)

where q'_{ms} and q'_{mt} are the mean heat transfer rates per unit surface area from the vertical cylindrical side surface of the cylinder and from the horizontal top surface of the cylinder, respectively.

Now, since

$$q'_{mc} A_c = q'_{ms} A_s + q'_{mt} A_t,$$ (2.5)

where A_c, A_s, and A_t are the surface areas of the entire cylinder, the vertical cylindrical side surface of the cylinder, and the horizontal top surface of the cylinder; it follows, using the previous equations, that:

$$Nu_{mc} = Nu_{ms} \left(\frac{A_s}{A_c} \right) + Nu_{mt} \left(\frac{A_t}{A_c} \right).$$ (2.6)

Therefore, since

$$A_s = 2\pi R h, \, A_t = \pi R^2, \text{ and } A_c = 2\pi R h + \pi R^2$$ (2.7)

it follows that

$$Nu_{mc} = Nu_{ms} \left(\frac{2}{R_d + 2} \right) + Nu_{mt} \left(\frac{R_d}{R_d + 2} \right),$$ (2.8)

where $R_d = R/h$.

This equation indicates that, as is to be expected, Nu_{mc} tends to Nu_{ms} at low values of R_d and that it tends to Nu_{mt} at large values of R_d.

A Rayleigh number based on the height of the cylinder and the overall temperature difference has been used in presenting the results, this Rayleigh number being defined as:

$$Ra = \frac{\beta g h^3 (T_w - T_F)}{\nu \alpha}.$$ (2.9)

2.2.2 Results

The solution has the following parameters:

- The Rayleigh number, Ra, as defined in the previous section, i.e., based on the height of the heated cylinder, h, and the overall temperature difference $T_w - T_F$,
- The dimensionless radius of the cylinder surface, $R_d = R/h$,
- The Prandtl number, Pr.

Fig. 2.4 Variation of mean Nusselt number for the cylinder with dimensionless cylinder radius for various values of the Rayleigh number (Oosthuizen PH 2007 ASME Paper IMECE2007-42711. By permission)
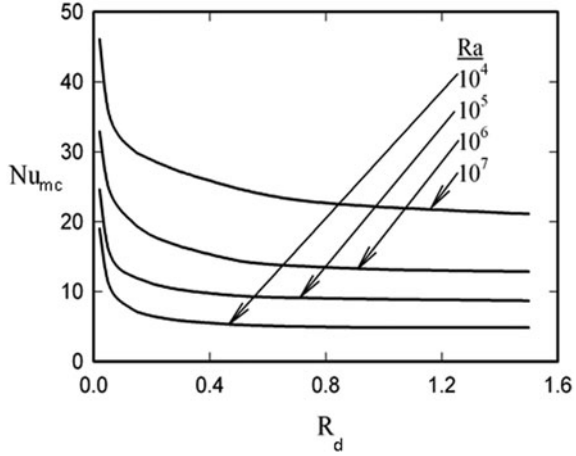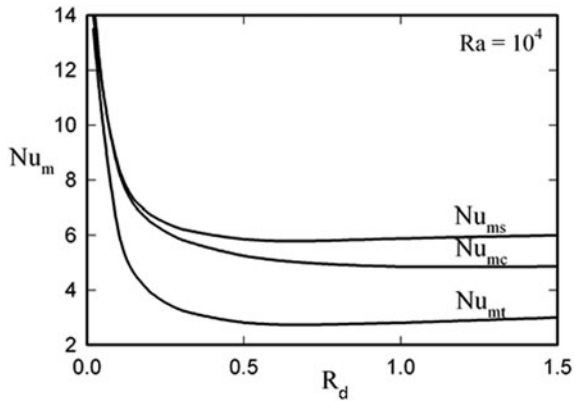

Fig. 2.5 Variation of mean Nusselt numbers for entire heated surface of the cylinder, for the vertical cylindrical portion of the cylinder, and for the top surface of the cylinder with dimensionless cylinder radius for $Ra = 10^4$ (Oosthuizen PH 2007 ASME Paper IMECE2007-42711. By permission)

As discussed in Chap. 1, because of the applications that motivated the studies described in this book, results were only obtained for $Pr = 0.74$, the approximate value for air at standard ambient conditions. A relatively wide range of the other governing parameters have been considered.

Typical variations of the mean Nusselt number for the entire cylinder surface, Nu_{mc}, with dimensionless cylinder radius R_d for various values of Ra are shown in Fig. 2.4. It will be seen that at low values of R_d at all considered values of Ra the Nusselt number increases sharply with decreasing R_d; whereas, at larger values of R_d the Nusselt number at a particular value of Ra is essential independent of R_d.

Attention will next be given to the mean Nusselt numbers for the side and top surfaces. Typical variations of Nu_{mc}, Nu_{ms}, and Nu_{mt} with R_d for four values of Ra are shown in Figs. 2.5–2.8. It will be seen from Figs. 2.5 to 2.8 that, as noted before, Nu_{mc} tends to Nu_{ms} at low values of R_d. This follows from the fact that much lower values of the Nusselt number, as is to be expected, will be seen to apply to the heated horizontal top surface than those that apply to the heated vertical side surface.

Fig. 2.6 Variation of mean Nusselt numbers for entire heated surface of the cylinder, for the vertical cylindrical portion of the cylinder, and for the top surface of the cylinder with dimensionless cylinder radius for $Ra = 10^5$ (Oosthuizen PH 2007 ASME Paper IMECE2007-42711. By permission)
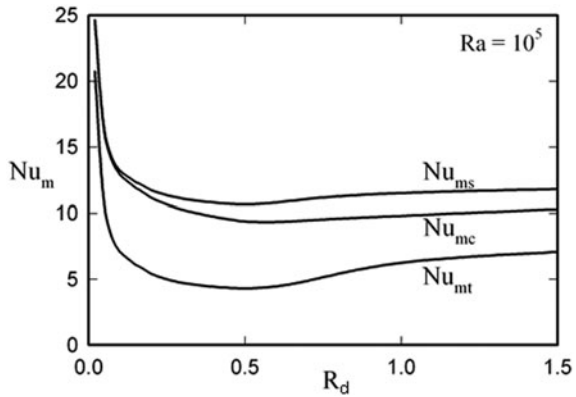
Fig. 2.7 Variation of mean Nusselt numbers for entire heated surface of the cylinder, for the vertical cylindrical portion of the cylinder, and for the top surface of the cylinder with dimensionless cylinder radius for $Ra = 10^6$ (Oosthuizen PH (2007) ASME Paper IMECE2007-42711. By permission)
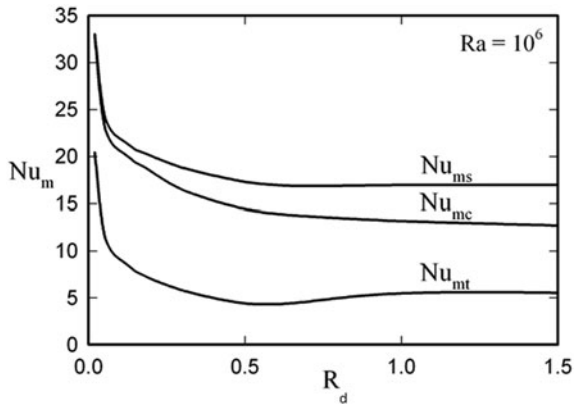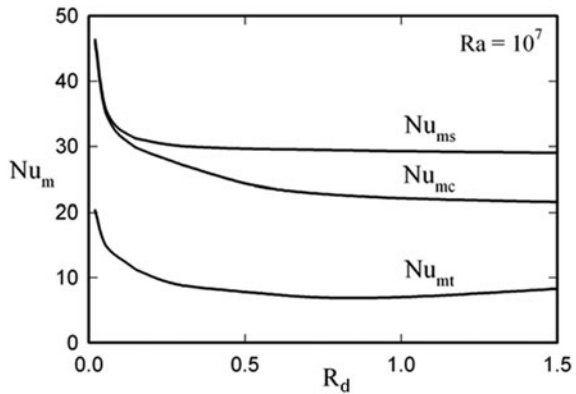
Fig. 2.8 Variation of mean Nusselt numbers for entire heated surface of the cylinder, for the vertical cylindrical portion of the cylinder, and for the top surface of the cylinder with dimensionless cylinder radius for $Ra = 10^7$ (Oosthuizen PH 2007 ASME Paper IMECE2007-42711. By permission)

This, together with the fact that the ratio of the area of the top surface to that of the side surface is equal to $R_d/2$, means that at low values of R_d the overall mean Nusselt number is essentially equal to the mean Nusselt number for the cylindrical side surface.

Now, one way of obtaining a correlation equation for Nu_{mc} is to develop correlation equations for Nu_{ms} and Nu_{mt} and then to use Eq. (2.8) to obtain the value of Nu_{mc}. Consider first the value of Nu_{ms}. Because Nu_{ms} must tend to the value for a vertical flat plate at larger values of R_d, it follows that since Eq. (2.10) applies for laminar flow over a wide vertical flat plate with a uniform surface temperature for a Prandtl number of 0.74:

$$\frac{Nu_m}{Ra^{0.25}} = 0.59 \tag{2.10}$$

the following can be assumed to apply for the cylindrical surface:

$$\frac{Nu_{ms}}{Ra^{0.25}} = 0.59 + \text{function}(R_d, Ra). \tag{2.11}$$

The second term on the right-hand side represents the effects of cylinder curvature. But curvature effects will depend on the ratio of the thickness of the boundary layer on the cylinder to the cylinder radius and since the boundary layer thickness is proportional to $h/Ra^{0.25}$ it follows that the ratio of boundary layer thickness to the cylinder radius will depend on the value of

$$\zeta = \frac{1}{R_d Ra^{0.25}}. \tag{2.12}$$

Therefore, Eq. (2.11) can be assumed to have the form:

$$\frac{Nu_{ms}}{Ra^{0.25}} = 0.59 + \text{function}\left(\frac{1}{R_d Ra^{0.25}}\right) = 0.59 + \text{function}(\zeta) \tag{2.13}$$

The numerical results given in Figs. 2.5–2.8 indicate that the function in Eq. (2.13) is approximately equal to 0.28ζ so Eq. (2.13) can be written as:

$$\frac{Nu_{ms}}{Ra^{0.25}} = 0.59 + 0.28\zeta \tag{2.14}$$

The results given by this equation are compared with the numerical results in Fig. 2.9 and satisfactory agreement will be seen to be obtained.

Equation (2.14) indicates that if it is assumed that curvature effects are negligible if the Nusselt number for the curved surface of the cylinder is within 1 % of the value for a vertical flat plate, then curvature effects are negligible if:

$$1 + \frac{0.28\zeta}{0.59} < 1.01, \text{ i.e., } \zeta < 0.021. \tag{2.15}$$

Consideration will next be given to the value of Nu_{mt}. Because the size of the horizontal top surface, i.e., its radius, will be the dimension that determines the heat transfer rate from this surface, the following Nusselt and Rayleigh numbers that use the radius as a length scale are defined:

$$Nu_{mtR} = Nu_{mt} R_d \text{ and } Ra_R = Ra R_d^3. \tag{2.16}$$

Fig. 2.9 Correlation of Nusselt number results for heat transfer from the vertical cylindrical portion of the cylinder (Oosthuizen PH 2007 ASME Paper IMECE2007-42711. By permission)
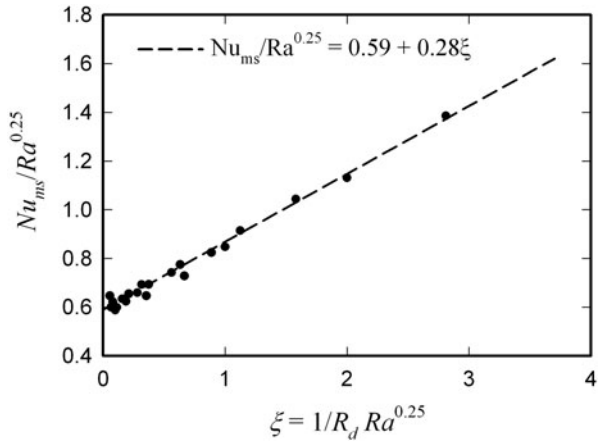
It has then been assumed that for the top surface for a specified Prandtl number $Nu_{mtR} = ARa_R^n$. Fitting an equation of this form to the numerical results given in Figs. 2.5–2.8 indicates that:

$$Nu_{mtR} = 0.45 Ra_R^{0.16}. \tag{2.17}$$

A comparison between the results given by this equation and the numerical results is shown in Fig. 2.10. The scatter in the results arises from the fact that there is some interaction of the flow up the heated vertical side surface and the flow over the heated top surface which is not directly accounted for here.

Equations (2.14), (2.16), and (2.17) together define Nu_{ms} and Nu_{mt}. Using the results given by these equations in Eq. (2.8) then allows Nu_{mc} to be found for any values of R_d and Ra. A comparison of the Nusselt values given by using this approach and the numerically determined Nusselt number values is shown in Fig. 2.11. The results given by the correlation equation will be seen to be in reasonably good agreement with the numerical results. Since the correlation equation has been derived by assuming that interaction between the flow over the vertical side cylindrical surface with the flow over the horizontal top surface is negligible, the adequacy of the fit between the correlation equation results and the numerical results indicates that this assumption is valid.

2.2.3   Experimental Results for a Vertical Isothermal Cylinder

Some very limited experimental results for natural convective heat transfer from short vertical cylinders mounted on a horizontal base with an exposed upper surface were obtained by Scott and Oosthuizen (2000). These results will be discussed in this section. More extensive experimental results will be given in Sect. 2.4 when

Fig. 2.10 Correlation of Nusselt number results for heat transfer from the horizontal top surface of the cylinder (Oosthuizen PH 2007 ASME Paper IMECE2007-42711. By permission)
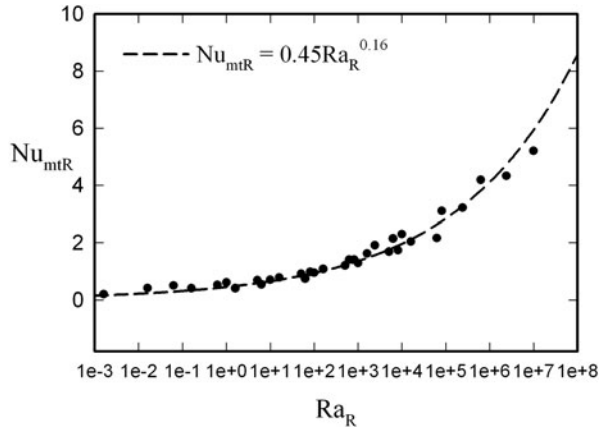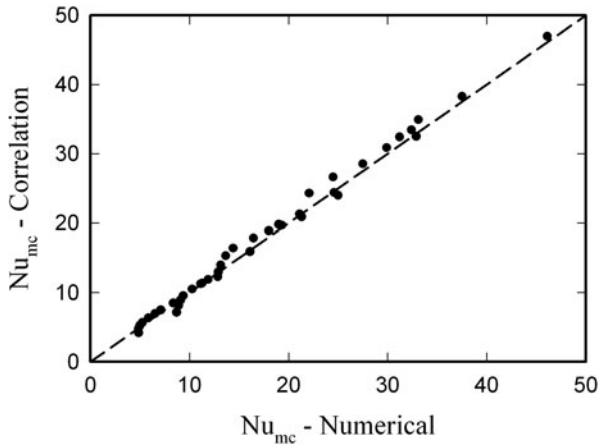
$$Nu_{mtR} = 0.45Ra_R^{0.16}$$

Fig. 2.11 Comparison of Nusselt number values given by correlation equation with the numerically obtained values (Oosthuizen PH 2007 ASME Paper IMECE2007-42711. By permission)

discussing results for an inclined cylinder, some of the results given in that section applying to a vertical cylinder.

As discussed in Chap. 1, mean heat transfer rates were determined using the transient lumped capacity method, i.e., by heating the model being tested and then measuring its temperature-time variation while it cooled. The models used were made from aluminum with a series of holes drilled into them from the bottom. Thermocouples inserted into these holes were used to measure the model temperature. In an actual test, the model being tested was heated in an oven to a temperature of about 90°C. It was then placed on the base plate which was made from Plexiglas. The model temperature variation with time was then measured while it cooled from approximately 80 to 40 °C. Because the Biot numbers existing during the tests were less than 1×10^{-3}, the temperature of the aluminum models remained effectively uniform at any given instant of time during the cooling process. The overall heat

transfer coefficient could then be determined from the measured temperature–time variation using the procedure discussed in Chap. 1.

The value of h_t so determined, as discussed in Chap. 1, is made up of the convective heat transfer to the surrounding air, the radiant heat transfer to the surroundings, and the conduction from the model to the base. The radiant heat transfer could be allowed for by calculation using the known emissivity value of the polished surface of the aluminum models.

The conduction heat transfer to the base was determined in separate tests in which the models were totally covered with thick Styrofoam insulation and by then using the transient method described previously to determine the value of the conduction heat transfer coefficient, h_{cd}.

The convective heat transfer coefficient could then be determined using:

$$h_c = h_t - h_r - h_{cd} \qquad (2.18)$$

In expressing the experimental results in dimensionless form, all air properties were evaluated at the mean film temperature $(T_{w_{avg}} + T_F)/2$ existing during the test.

The uncertainty in the experimental values of Nusselt number arises due to uncertainties in the temperature measurements, in the corrections applied for conduction heat transfer to the base, and small temperature differences in the model during cooling. Therefore, an uncertainty analysis was performed by applying the Moffat (1983, 1988) method. This indicated that the uncertainty in the measured Nusselt number was less than $\pm 12\%$.

Tests were performed with models having the dimensions shown in Table 2.1.

Figure 2.12 shows a typical comparison between the experimental results and the Nusselt number variations given by using the correlation equations based on the numerical results that were discussed in the previous section. It will be seen that the experimental results agree with those determined using the numerical results to within the experimental uncertainty.

2.2.4   Concluding Remarks

The results given in this section indicate that:

1. For an upward pointing cylinder with an exposed upper surface the mean Nusselt number for the heated top horizontal surface is much lower than that for the heated vertical side surface. This, together with the fact that the area of the top surface at the lower values of R_d considered is much less than the area of the side surface, means that the heated side surface is dominant in determining the overall mean Nusselt number. A rough guide is that if R_d is less than 0.1, the heat transfer from the top surface is essentially negligible.
2. Curvature effects on the Nusselt number for the vertical cylindrical side surface are negligible if $\zeta < 0.021$.

http://www.springer.com/978-3-319-02458-5

Natural Convective Heat Transfer from Short Inclined
Cylinders
Oosthuizen, P.H.; Kalendar, A.
2014, VII, 128 p. 139 illus., Softcover
ISBN: 978-3-319-02458-5